Available at www.sciencedirect.com

ScienceDirect

journal homepage: www.elsevier.com/locate/watres

Monitoring off-gas O_2/CO_2 to predict nitrification performance in activated sludge processes

Shao-Yuan Leu [a], *Judy A. Libra* [b], *Michael K. Stenstrom* [a,*]

[a] *Environmental Engineering Department, University of California, Los Angeles, CA 90095, USA*
[b] *Institut Verfahrenstech, Technische Universität Berlin, Berlin 10623, Germany*

ARTICLE INFO

Article history:
Received 6 October 2009
Received in revised form
23 January 2010
Accepted 20 March 2010
Available online 27 March 2010

Keywords:
Wastewater
Activated sludge process
Off-gas
Dynamic model
Nitrification

ABSTRACT

Nitrification/denitrification (NDN) processes are the most widely used technique to remove nitrogenous pollutants from municipal wastewater. The performance of nitrogen removal in the NDN process depends on the metabolism of nitrifying bacteria, and is dependent on adequate oxygen supply. Off-gas testing is a convenient and popular method for measuring oxygen transfer efficiency (OTE) under process conditions and can be performed in real-time. Since carbon dioxide is produced by carbonaceous oxidizing organism and not by nitrifiers, it should be possible to use the off-gas carbon dioxide mole fraction to estimate nitrification performance independently of the oxygen uptake rate (OUR) or OTE. This paper used off-gas data with a dynamic model to estimate nitrifying efficiency for various activated sludge process conditions. The relationship among nitrification, oxygen transfer, carbon dioxide production, and pH change was investigated. Experimental results of an online off-gas monitoring for a full-scale treatment plant were used to validate the model. The results showed measurable differences in OUR and carbon dioxide transfer rate (CTR) and the simulations successfully predicted the effluent ammonia by using the measured CO_2 and O_2 contents in off-gas as input signal. Carbon dioxide in the off-gas could be a useful technique to control aeration and to monitor nitrification rate.

1. Introduction

Nitrification/denitrification (NDN) in the activated sludge process (ASP) is the state of the art technique to remove nitrogenous pollutants in municipal wastewater. The activated sludge process consists of many different types of active bacteria, often called "active mass" in structured ASP models (Clifft and Andrews, 1986), which can have a wide range of biodegradation mechanisms for different types of pollutants. Consumption of carbonaceous compounds and denitrification are generally performed by heterotrophic bacteria, and nitrification is performed by autotrophic bacteria. The performance of an ASP is highly dependent on the operating conditions. In aeration basins, many criteria must be carefully maintained to provide a suitable habitat for microorganisms, especially for nitrifiers, such as proper pH, temperature, (Painter, 1970; Painter and Loveless, 1983), adequate solids retention time (SRT, Poduska and Andrews, 1975), and sufficient dissolved oxygen (DO) concentration (Stenstrom and Poduska, 1980).

Nitrification failure can easily occur under low DO conditions, which are controlled by a number of factors, such as oxygen transfer efficiency (OTE) and the overall oxygen uptake rate (OUR, Stenstrom and Song, 1991). The off-gas test described by Redmon et al. (1983) can be used to estimate process water oxygen transfer status for aeration systems

* *Corresponding author*. Tel.: +1 310 825 1408; fax: +1 310 206 2222.
E-mail address: stenstro@seas.ucla.edu (M.K. Stenstrom).
0043-1354/$ – see front matter © 2010 Elsevier Ltd. All rights reserved.
doi:10.1016/j.watres.2010.03.022

Nomenclature

CH_xO_y	empirical formula of carbonaceous substrate
CO_2	CO_2 mole fraction in off-gas (mole/L)
CTR	CO_2 transfer rate (kg/day)
CUR	CO_2 uptake rate (kg/day)
H_{CO2}	Henry's constant (mole CO_2/mg $H_2CO_3^*$)
S	carbonaceous substrate (mg/L)
S^{∞}	saturated dissolved gas concentration (mg/L)
S_O	dissolved oxygen concentration (mg/L)
S_{NH}	ammonia (mg-N/L)
K_1, K_2	CO_2 dissociation constants
K_D	decay coefficient (1/day)
K_S	half-velocity coefficient of substrate (mg/L)
K_N	half-velocity coefficient of nitrification (mg/L)
K_O	half-velocity coefficient of DO (mg/L)
O_2	O_2 mole fraction in off-gas (mole/L)
OTR	oxygen transfer rate (kg/day)
OUR	oxygen uptake rate (kg/day)
Q_g	air flow rate (m^3/day)
Q_l	volumetric flow rate (m^3/day)
V	volume (m^3)
X_H	concentration of heterotrophic bacteria (mg COD/L)
X_I	concentration of inert biomass (mg COD/L)
X_N	concentration of autotrophic bacteria (mg COD/L)
X_{STO}	concentration of stored mass (mg COD/L)
Y	yield coefficient (g COD biomass/g COD substrate)
$\overline{Y}$	molar yield (mole biomass/mole substrate)
$\alpha K_L a$	oxygen transfer coefficient under processing conditions (1/day)
$\alpha K_L a_{CO2}$	CO_2 transfer coefficient under processing conditions (1/day)
δ	storage coefficient
μ_{max}	maximum specific heterotrophic growth rate (g COD/g COD-day)
μ_N	maximum specific autotrophic growth rate (g COD/g N-day)
f_{XI}	fraction inert biomass from decayed cells (g COD/g COD)
$f_{H_2CO_3}$	fraction bicarbonate over total dissolved CO_2
$r_{HCO_3^-}$	transfer rate to bicarbonate (kg/hour)
k_1, k_2	CO_2 transformation kinetics
k_{sto}	specific reaction rate of substrate stored reaction (g COD/g COD-day)

Subscripts or superscripts

C	carbonaceous oxidation reaction
D	cell decay reaction
$H_2CO_3^*$	dissolved carbon dioxide
HCO_3^-	bicarbonate
H,S	direct synthesis of heterotrophic biomass
H,STO	heterotrophic growth on stored mass
IN	influent conditions
O	for dissolved oxygen
N	ammonia oxidation reaction, nitrification
NH	for ammonia
STO	stored mass

(Rosso et al., 2005), and has been widely used to test aeration basins under process conditions (American Society of Civil Engineering, ASCE, 1997). The off-gas analyzer and testing procedure can also be used to measure other gas fractions (nitrogen, carbon dioxide, water vapor, volatile organic chemicals), but it is commonly used to measure only oxygen mole fraction. The CO_2 mole fraction can be easily measured if an additional analyzer, such as a CO_2 absorption tube or infrared sensor is used.

Because the reaction by-products of carbonaceous and nitrogenous compounds are different, the relative amounts of CO_2 produced and oxygen consumed can become the basis for a new method of analyzing nitrification rate: the molar fraction of carbon dioxide in the off-gas should be greater if nitrification is limited, or the fraction of nitrogenous compounds of the total oxygen demand is less.

The main problem of the proposed method is the "supersaturatation" of dissolved carbon dioxide due to change of pH. At normal pH, carbon dioxide concentration in gas phase is a function of dissolved CO_2 concentration, influent alkalinity, and pH. When pH changes, dissolved carbon dioxide acts as a buffer and shifts the fraction between carbonic acid (H_2CO_3) and bicarbonate (HCO_3^-) to consume or release hydrogen ions. Since CO_2 transfer relates to the concentration of carbonic acid, increasing the fraction of bicarbonate creates a supersaturated condition until the dissolved CO_2 can be stripped. Stripping of CO_2 also leads to an increase in pH, which shifts the equilibrium towards bicarbonate and similar to the response of receiving high alkalinity influents. Hellinga et al. (1996) calculated the ratio of carbon dioxide production rate (CPR) and oxygen uptake rate (OUR) for different wastewater compositions. The authors demonstrated that off-gas measurements are useful for evaluating the reactivity of carbonaceous substrate (i.e. COD/TOC ratio), because the changes of CPR are small due the buffering capacity of bicarbonate equilibrium. Similar discussions were also presented by others (Nogita et al., 1982; Minkevich and Neubert, 1985; Spérandio and Paul, 1997).

Experimental and modeling studies have evaluated or simulated the supersaturated conditions of dissolved CO_2 in bioreactors. Pratt et al. (2003, 2004) used a titrimetric technique with off-gas analysis, called on-line titrimetric and off-gas analysis (TOGA), to calculate the effect of changing pH in batch systems. Hydrogen ion production rate (HPR) was measured by monitoring the shift of pH due to *in-situ* titration, and CPR was monitored in the off-gas using a mass spectrometer. By knowing HPR and CPR, the transfer rates of oxygen, nitrogen and carbon dioxide were calculated from stoichiometry. Weissenbacher et al. (2006) proposed a simplified model to take account the effect of pH shift or change in alkalinity to off-gas CO_2 mole fraction. Instead of simulating alkalinity and pH shift, the authors used on-line pH measurements as input signals to experimentally evaluate CPR. This modeling approach is similar to what is used in this paper.

Goals of this paper are to understand the relationships of CO_2 and O_2 in off-gas emissions and to develop a method for estimating nitrification efficiency of a full-scale ASP bioreactor

based upon off-gas O_2/CO_2 monitoring. A mathematical model was built to simulate the temporal concentrations of the major components in wastewater and off-gas, and results of field measurements were applied to validate the model. Online off-gas tests were performed in a full-scale wastewater treatment plant, and the relationships between oxygen uptake/transfer, carbon dioxide production/transfer, change of pH, and nitrification performance were investigated. The model was used to create a profile between off-gas O_2/CO_2 and reaction status of carbonaceous substrate/ammonia, in order to study the effects of changing pH to CO_2 stripping, and to simulate/predict ammonia discharge.

2. Materials and methods

2.1. Off-gas test

A floating hood on the surface of the aeration basinas was used to collect off-gas and the mole fractions of oxygen and carbon dioxide were measured. In the ASCE (1997) Standard Guidelines for Process Water Testing, oxygen transfer efficiency (OTE, %) is calculated by comparing the oxygen content in the supplied air and the off-gas. If clean water transfer efficiency is known, the alpha factor (α) can be calculated as the ratio of the OTE in process water, adjusted to standard conditions, to the OTE in clean water. The off-gas flow rate or flux and total air flow can also be determined using air flow rate captured by the hood, hood area and tank surface area. Iranpour and Stenstrom (2001) discussed the relationship between oxygen transfer rate and air flow in more detail.

The oxygen transfer rate (OTR, Kg O_2/hour) is the product of OTE and off-gas flow rate, and can be compared to clean water data and other conditions by calculating the αSOTE or αSOTR by adjusting to standard conditions (20 °C, 0 mg/L of dissolved oxygen, 1 atm, 0 salinity), with the exception of the α factor, using the relationships described in the ASCE (2006, 1997) standards and Stenstrom et al. (1989). The OTR is calculated as follows:

$$\mathrm{OTR} = Q_g^{\mathrm{HOOD}} \frac{O_2^{\mathrm{IN}} - O_2^{\mathrm{OUT}}}{O_2^{\mathrm{IN}}} \times \frac{\mathrm{Area}^{\mathrm{TANK}}}{\mathrm{Area}^{\mathrm{HOOD}}} \quad (1)$$

The carbon dioxide transfer rate (CTR, Kg/hour) is calculated by a similar fashion:

$$\mathrm{CTR} = Q_g^{\mathrm{HOOD}} \frac{CO_2^{\mathrm{OUT}} - CO_2^{\mathrm{IN}}}{CO_2^{\mathrm{IN}}} \times \frac{\mathrm{Area}^{\mathrm{TANK}}}{\mathrm{Area}^{\mathrm{HOOD}}} \quad (2)$$

2.2. Background of investigated wastewater treatment plant

Field experiments were performed in the wastewater treatment plant of Waßmannsdorf, Germany. Table 1 shows the wastewater composition and operational properties of the tested plant. The plant is a medium size NDN plant with capacity of approximately 31,000 m^3/day (8.2 MGD). The aerobic zone volume is 13,450 m^3, or 53% of the total aeration tank volume. Aeration tank was equipped with fine-pore diffusers and the air flow rate was controlled by conventional constant-DO control systems. The average influent total COD is approximately 600 mg/L and the ammonia concentration is approximately 50 mg-N/L. Fig. 1 shows the schematic diagram of the wastewater treatment process and the sampling locations.

Table 1 – Wastewater composition and operation conditions of the tested treatment plant.

Property	Range	Mean
Plant flow, m^3/hour	550–1900	1,350
Total COD, mg/L	467–808	600
Soluble COD, mg/L	195–386	280
Ammonia, mg-N/L	41.0–58.4	50
Organic-Nitrogen, mg-N/L	11.6–20.4	15
MLVSS, mg/L	3000–4200	3600

Off-gas tests were performed by a conventional off-gas analyzer which continuously receives off-gas stream from three fixed hoods (Fig. 2(b)), and carbon dioxide content was measured by an infrared sensor (Schuchardt et al., 2005). The conventional off-gas analyzer has been described by Redmon et al. (1983) and can be improved for real-time or online monitoring (Leu et al., 2009). The analyzer recorded hood air flux and oxygen and carbon dioxide mole fraction once every 2 h. The 2-h testing interval should be sufficient enough for monitoring nitrogen removal, since the hydraulic retention time for the aerobic zone is between 7 and 24 h. Measured data from four different seasons were chosen for this study, and each of the periods continued at least 10 days. Time-series influent and effluent conditions were monitored during the testing period for model calibration, recording parameters of plant flow, COD, ammonia, nitrate, DO, MLVSS, and pH.

2.3. Activated sludge model

The activated sludge model is based on the Cliff and Andrews (1986), and Poduska and Andrews (1975) models which are similar to the carbonaceous and nitrification/denitrification parts of general Activated Sludge Models No. 3 (ASM3, Gujer et al., 1999). One difference between our approach and ASM3 is a pathway for direct growth of active biomass from soluble substrate, which provides for simultaneous growth from substrate and stored mass, which Krishna and van Loosdrecht (1999) have suggested better describes the real conditions of the growth of heterotrophic bacteria. For convenience we used parameter, δ, (Sin et al., 2005) to define the yield coefficients of direct heterotrophic growth ($Y_{H,S}$), substrate storage (Y_{STO}), and heterotrophic growth ($Y_{H,STO}$) on stored mass as:

$$Y_{H,S} = \frac{4\delta - 2}{4.2\delta + 4.32} \times \frac{4.2}{4}, \quad Y_{STO} = \frac{4\delta - 2}{4.5\delta} \times \frac{4.5}{4}, \quad \text{and}$$
$$Y_{H,STO} = \frac{4.5\delta - 0.5}{4.2\delta + 4.32} \times \frac{4.2}{4.5} \quad (3)$$

The model simulates the temporal concentrations of carbonaceous substrate (S), stored mass (X_{STO}), heterotrophic (X_H), autotrophic (X_N), and inert biomass (X_I) in the biological phase; dissolved oxygen (S_O), carbon dioxide (S_{H2CO3^*}), ammonia (S_{NH}), and nitrate (S_{NO}) in the liquid phase; and oxygen (O_2), carbon dioxide (CO_2) contents in the gas phase. To accurately calculate the mass production/consumption of

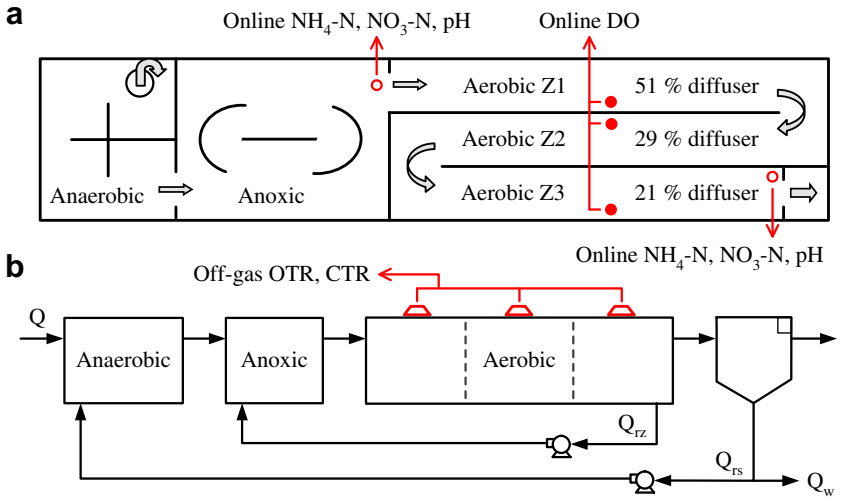

Fig. 1 – (a) Tank geometry and (b) schematic diagram of tested wastewater treatment plant (Waβmannsdorf, Berlin, Germany). Symbols show the monitored parameters and sampling locations.

each simulated compound, stoichiometry was derived for all reactions. In this model, all forms of carbonaceous substrates (rapidly degradable COD, slowly degradable COD, or stored COD) are expressed as CH_xO_y with constant x, y, stored mass is C_2H_3O, and $C_5H_7NO_2$ is used for all bacteria species (heterotrophic or nitrifying bacteria). The values of x and y were originally unknown and then validated with whole plant mass balance. The five reactions which occur simultaneously in the reactor are: (1) storage of carbonaceous substrate; (2) the direct growth of heterotrophic biomass; (3) growth of

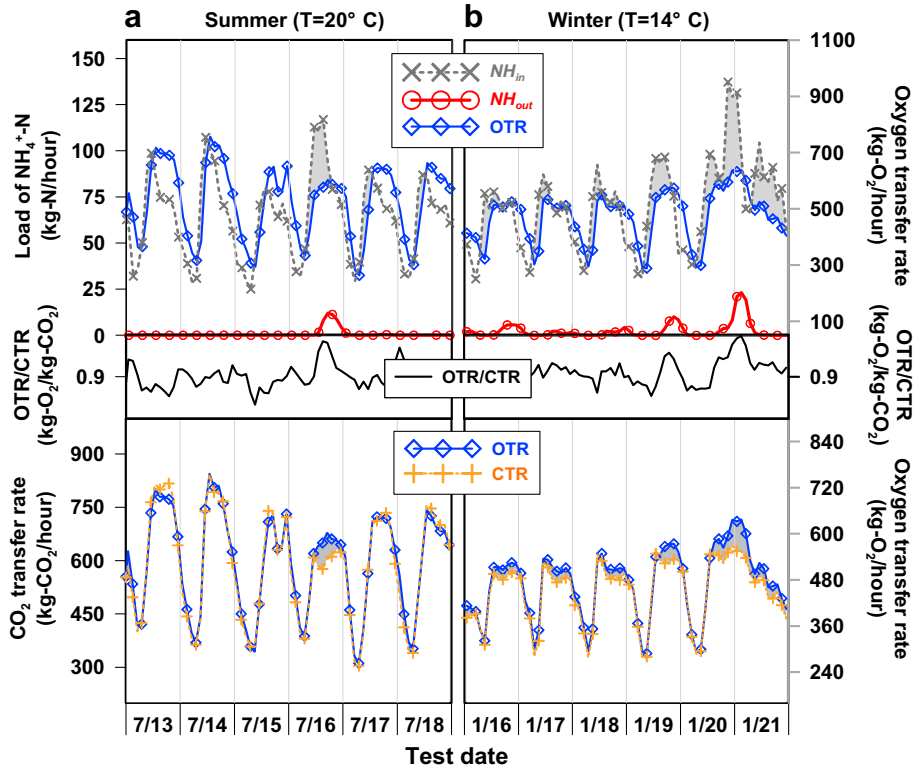

Fig. 2 – Experiment results of real-time off-gas tests and nitrification status in a full-scale ASP. Two columns shows the data collected from two seasons: (a) summer with average temperature of 20°C; and (b) winter of 14 °C. Nitrification status versus oxygen transfer rate (OTR) measured by off-gas tests is plotted on the top rows; carbon dioxide transfer rate (CTR) compared to OTR is plotted on the bottom; in the middle is the OTR/CTR ratio. Difference between CTR and OTR can be observed at NH_4^+ break period.

heterotrophic biomass on stored mass; (4) nitrification; and (5) biomass decay. The stoichiometry of each reaction can be expressed as follows:

Storage of carbonaceous substrate:

$$CH_xO_y + \left(1 + \frac{x}{4} - \frac{y}{2} - \frac{9}{4}\overline{Y}_{STO}\right)O_2 \rightarrow \overline{Y}_{STO}C_2H_3O + (1 - 2\overline{Y}_{STO})CO_2 + \left(\frac{x}{2} - \frac{3}{2}\overline{Y}_{STO}\right)H_2O \quad (4)$$

Growth of heterotrophic bacteria (direct or growth on stored mass using $x = 1.5$, $y = 0.5$):

$$CH_xO_y + \overline{Y}NH_4^+ + \left(1 + \frac{x}{4} - \frac{y}{2} - 5\overline{Y}\right)O_2 \rightarrow \overline{Y}C_5H_7NO_2 + (1 - 5\overline{Y})CO_2 + \left(\frac{x}{2} - 2\overline{Y}\right)H_2O + \overline{Y}H^+ \quad (5)$$

Nitrification:

$$NH_4^+ + 5\overline{Y}_NCO_2 + (2 - 7\overline{Y}_N)O_2 \rightarrow \overline{Y}_NC_5H_7NO_2 + (1 - \overline{Y}_N)NO_3^- + (2 - \overline{Y}_N)H^+ + (1 - 3\overline{Y}_N)H_2O \quad (6)$$

Endogenous respiration or biomass decay:

$$C_5H_7NO_2 + 5O_2 + H^+ \rightarrow 5CO_2 + 2H_2O + NH_4^+ \quad (7)$$

Table 2 shows the kinetics and the simulated components in a matrix form similar to the IWA ASM. The mass balance equations can be developed by adding the product of the coefficients listed in the column and the process rate of each reaction in the right end column. The coefficients in each column are calculated from stoichiometry, and Monod functions are assumed to describe various cell growth criteria. Simulations of dissolved oxygen (DO) and carbon dioxide shown in the next section provide examples of using the proposed model structure.

2.4. Simulation of gas transfer

The DO mass balance uses the oxygen uptake rate (OUR) of heterotrophic growth and decay and nitrification and oxygen transfer rate (OTR). In this paper, OTR represents the gas transfer capacity of aeration system, and OUR is the mass oxygen consumed to degrade certain pollutants per unit volume, i.e. nitrification (OUR_N), oxidation of carbonaceous substrate (OUR_C), and cell decay (OUR_D). The mass balance of DO can be expressed as:

$$V\frac{dS_O}{dt} = \frac{Q_l}{V}(S_O^{IN} - S_O) + OTR - OUR_N - OUR_C - OUR_D \quad (8)$$

In the model, simulation of oxygen transfer across the gas/liquid interfaces is based on the well-known two film theory (Lewis and Whitman, 1924), which can be expressed as:

$$OTR = \alpha K_L a \times V \times (S_O^{\infty} - S_O) \quad (9)$$

OUR_C, OUR_N, and OUR_D represent the oxygen consumption for substrate degradation, nitrification, and biomass decay, respectively. The oxygen uptake to consume a unit mass of substrate is calculated by multiplying the growth rate with appropriate stoichiometric yields. Table 2 shows all the required parameters and the following example is given to illustrate how the OUR (in this case for nitrification) is written as:

$$OUR_N = Y_O^{NH}\,\mu_N\frac{S_{NH}}{K_N + S_{NH}} \times \frac{S_O}{K_O + S_O}X_N\,V \quad (10)$$

In Eq. (10) Y_O^{NH} is the oxygen demand of ammonia oxidation by nitrifiers and is derived from Eq. (6). The relationship between Y_O^{NH} (g O_2/g COD nitrifying biomass) and molar yield $\overline{Y}_N$ can be expressed as:

Table 2 – Model matrix of yield coefficient and model kinetics.

	Reactions	S	S_{NH}	X_{STO}	X_H	X_N	X_I	S_O	S_{H2CO3^*}	S_{HCO3-}	Reaction kinetics (mg/L/day)
		gCOD	gN	gCOD	gCOD	gCOD	gCOD	gO_2	gCO_2	gCO_2	
1	Storage of carbonaceous substrate	$\frac{-1}{Y_{STO}}$		1				$-Y_O^{STO}$	$Y_{CO_2}^{STO}$		$k_{sto} \times M_O \times M_S \times X_H$
2	Direct synthesis of heterotrophic bacteria	$\frac{-1}{Y_{H,S}}$	$-Y_{NH}^{H,S}$		1			$-Y_O^{H,S}$	$Y_{CO_2}^{H,S}$		$\mu_{max,S} \times M_S \times M_O \times M_{NH} \times X_H$
3	Heterotrophic growth on stored mass		$-Y_{NH}^{H,STO}$	$\frac{-1}{Y_{H,STO}}$				$-Y_O^{H,STO}$	$Y_{CO_2}^{H,STO}$		$\mu_{max,sto} \times M_S \times M_O \times M_{NH} \times \frac{f_{sto}^2}{K_{sto2} + f_{sto} \times K_{sto1}}X_H$
4	Nitrification		$\frac{-1}{Y_N}$			1		Y_O^{NH}	$-Y_{CO_2}^{NH}$		$\mu_N \times M_{NH,N} \times M_{O,N} \times X_N$
5	Endogenous respiration		Y_{NH}^X		-1		f_{XI}	$-(1 - f_{XI})$	$Y_{CO_2}^X$		$K_D \times X_H$
6	Oxygen transfer							1			$\alpha K_L a(S_O^{\infty} - S_O)$
7	Carbon dioxide transfer								1		$\alpha K_L a_{CO_2}(S_{H_2CO_3^*}^{\infty} - S_{H_2CO_3^*})$
8	Bicarbonate equilibrium								-1	1	$(k_1 + k_2 \times 10^{pH-14})S_{H_2CO_3^*} - (k_{-2} + k_{-1} \times 10^{pH}) \cdot S_{HCO_3^-}$

Note: $f_{sto} = X_{STO}/X_H$; $f_{H_2CO_3} = S_{H_2CO_3^*}/(S_{H_2CO_3^*} + S_{HCO_3^-} + S_{CO_3^{2-}})$; $M_S = S_S/(K_S + S_S)$; $M_O = S_O/(K_O + S_O)$; $M_{NH} = S_{NH}/(K_N + S_{NH})$.

$$Y_O^{NH} = \frac{2 - 7\overline{Y}_N}{\overline{Y}_N} \times \frac{32}{113} \times \frac{1}{1.42} \quad (11)$$

Oxygen demands of heterotrophic and endogenous respiration are calculated in a similar fashion. By combining all reactions to Eq. (8), transient DO and OTR can be simulated.

Simulation of carbon dioxide transfer is more complex than oxygen due to the bicarbonate equilibrium. In additional to the reaction kinetics described by the bacteria activities, such as carbon dioxide uptake for autotrophic growth (CUR), production due to heterotrophic growth and biomass decay (CPR), and the CO_2 transfer rate (CTR), an additional mass balance and reaction term were needed to determine the pH. The relationships among dissolved carbon dioxide (S_{H2CO3^*}), bicarbonate (S_{HCO3^-}), and the off-gas CO_2 (CO_2) can be derived as:

$$V\frac{dS_{H_2CO_3^*}}{dt} = Q_l\left(S^{IN}_{H_2CO_3^*} - S_{H_2CO_3^*}\right) - CTR - CUR_N + CUR_C + CUR_D - r_{HCO_3^-} \quad (12)$$

$$V\frac{dS_{HCO_3^-}}{dt} = Q_l\left(S^{IN}_{HCO_3^-} - S_{HCO_3^-}\right) + r_{HCO_3^-} \quad (13)$$

$$V\frac{dCO_2}{dt} = Q_g\left(CO_2^{IN} - CO_2\right) + CTR \quad (14)$$

Spérandio and Paul (1997) estimated the transformation rate of bicarbonate ($r_{HCO_3^-}$) using the CO_2 transformation kinetics (k_1, k_2) and the CO_2 dissociation constants (K_1, K_2), which can be expressed as:

$$r_{HCO_3^-} = V\left[\left(k_1 + k_2 \times 10^{pH-14}\right)S_{H_2CO_3^*} - \left(k_2 + k_{-1} \times 10^{pH}\right) \times S_{HCO_3^-}\right] \quad (15)$$

where $k_{-1} = k_1/K_1$; $k_{-2} = k_2/K_2$.

The concentration of bicarbonate and dissolved CO_2 ($H_2CO_3^*$) changes with pH: when pH decreases, bicarbonate gains proton and transformed to dissolved CO_2, whereas increase CO_2 stripping, and vise versa. If pH shift is too significant, off-gas CO_2 measurements may be upset. Fortunately, biological treatment processes requires and is normally controlled at constant pH, the changes of CO_2 transfer due to pH shifting should be small. Based on this assumption, modeling efforts can be applied to correct the off-gas measurements of CO_2. In this study, pH changes associated with periodical plant alkalinity measurement was used as input signal to adjust the CO_2 simulation.

CTR is simulated in a similar fashion as OTR and the mass transfer coefficient ($\alpha K_L a_{CO2}$) was calculated based on the $\alpha K_L a$ of O_2 measured by off-gas tests. The saturated concentration $S^{\infty}_{H_2CO_3^*}$ can be calculated by Henry's Law; whereas all the relationships can be expressed as:

$$CTR = \alpha K_L a_{CO_2} V\left(S^{\infty}_{H_2CO_3^*} - S_{H_2CO_3^*}\right) \quad (16)$$

$$\alpha K_L a_{CO_2} = 0.91\alpha K_L a \quad (17)$$

$$S^{\infty}_{H_2CO_3^*} = H_{CO_2}CO_2 \quad (18)$$

The model was programmed using Matlab 7.0 (MathWorks, Natick, Massachusetts) using a fourth-order correct, variable-time-step Runge-Kutta technique (function ode45) to integrate the mass balance ordinary differential equations (ODEs). The model simulates five microbial reactions, two gas transfer functions, and the bicarbonate equilibrium (Table 2).

2.5. *Model calibration*

To develop the model, a steady-state mass balance based upon the overall long-term measurements was performed to investigate the fates of "carbon-" and "oxygen-" compounds (calculated from transfer rate, kg-O_2/hour and kg-CO_2/hour) in the aeration tank and to evaluate certain model parameters, i.e. the composition of carbonaceous compounds and yield coefficients of by-products. The long-term averaged data, including plant loads, off-gas data, online DO, and sludge wasting rate, were used to calculate the total CO_2 in the liquid phase. For example, carbon enters the system from influent substrate, and is converted to biosolids, carbon dioxide in the off-gas, and dissolved carbon dioxide. The dissolved carbon dioxide can be calculated by difference. The oxygen balance was performed in a similar fashion. From this information, the pH and alkalinity balance can then be applied to evaluate the effect of super-saturation (based on equations (4)–(8) and (12)–(14)).

Monod kinetics and other model parameters were validated by matching the simulation results with measurement data. The model assumed a well mixed aeration tank and the off-gas data were the flow-weighted average of three hood positions; simulation of hydraulic conditions was not required. The least squares difference of simulated and measured ammonia concentration (S_{NH}), oxygen and carbon dioxide molar fraction (O_2 and CO_2) were compared to select the set of best-fit parameters. The calibration approach is similar to former studies of Tzeng et al. (2003) and Yuan et al. (1993), who calibrated models for full-scale, high purity oxygen (HPO) plants from off-gas data associated with liquid phase experiment results. The validated model was then used to study the effects of pH shifting and to simulate nitrification performance.

Table 3 – Average plant monitoring and results of off-gas tests.

Property	Symbol	Unit	Testing period			
			1-May	2-July	3-Nov	4-Jan
Temperature	T	°C	19.8	21.5	17.1	14.0
Solid retention time	SRT	day	7.9	8.0	11.0	15.5
Average DO	S_O	mg/L	1.4	1.5	1.6	1.7
Effluent NH_4^+–N	S_{NH}	mg-N/L	0.25	0.27	0.47	1.15
Gas transfer coefficient	$\alpha K_L a$	1/hour	4.5	4.4	4.3	4.0
Oxygen transfer rate	OTR	kg/hour	584	488	490	464
Carbon dioxide transfer rate	CTR	kg/hour	584	553	545	499

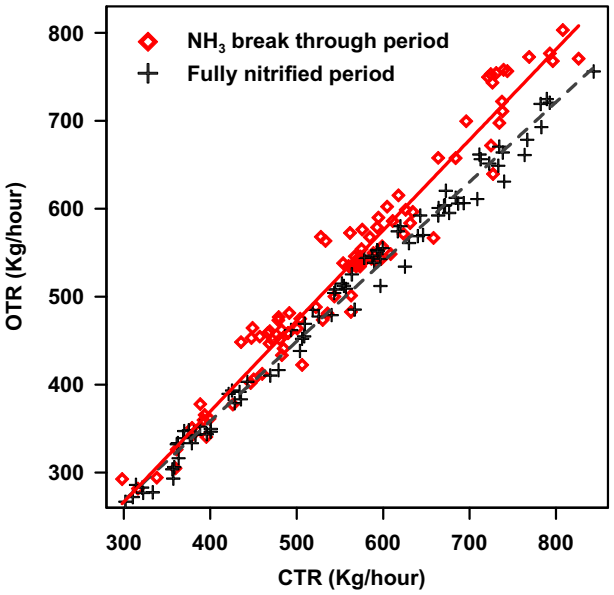

Fig. 3 – Correlations of off-gas measured CTR and OTR at ammonia overloading period and fully nitrified period. Distinguishable higher OTR can be observed during the ammonia breakthrough period.

3. Results and discussion

3.1. *Primary analyses of off-gas data*

Table 3 shows the operating conditions and the average measurement data during the four testing periods. The average DO and off-gas data are relatively constant during the year, but the solids retention time (SRT) was changed in response to water temperature changes. SRT increased from approximately 8 days in summer to 15.5 days in winter to provide better nitrification. Fig. 2 shows the results of online off-gas monitoring and nitrification conditions. Examples of two testing periods are shown: (a) summer time with average liquid temperature of 20 °C and SRT= 8 days; and (b) winter time with temperature of 14 °C and SRT=15.5 days. The upper panels compares the OTR and the plant nitrogen load shown as mass of nitrogen feed per hour; the middle panel shows the ratio of OTR and CTR; and the lower panel compares the OTR and CTR. Note that the Y-axis scale for OTR in the lower panel was expanded to emphasize the differences in CRT and OTR.

The plant fully nitrified during most of the summer except one or two days when the loadings were extremely high. During the winter nitrification was less consistent, with minor break through at several times. The results of OTR basically follow the plant loading except at high nitrogen loading period, and with a consistent 2–3 h lag. The plant uses a conventional DO control system to control total air flow, therefore it is reasonable OTR is proportional to the total plant loadings when all pollutants are fully oxidized. One important observation between OTR measurement and nitrogen loadings is the nitrification limit. At high loading period (upper panel, shaded area with high influent nitrogen load, date 7/17, 1/20, and 1/21), ammonia was discharged. This observation served as a good example of the real-time OTR monitoring since DO was still at constant (~1.9 mg/L) during this period and did not provide information about nitrification shortfall.

The ratios of OTR/CTR over the testing period were plotted in the middle panel of Fig. 2, which showed that OTR/CTR ratio changed with nitrification conditions. The measured CTR and

Table 4 – Steady-state mass balance of carbon and oxygen.

Transfer rate of compounds	In	Out
Carbon (kg-C/hour)		
Total substrate (CH_xO_y)	+455.5	
Biosolids wastage ($C_5H_7NO_2$)		−218.1
Gas transfer out as CO_2		−144.8
Discharged liquid phase CO_2		92.6
Oxygen (kg-O_2/hour)		
Total substrate (CH_xO_y)	+289.8	
Gas transfer in as O_2	+492.8	
Gas transfer out as CO_2		−386.2
Biosolids wastage ($C_5H_7NO_2$)		−116.3
Discharged DO		−2.2
Discharged NO_3		−33.1
Discharged liquid phase CO_2		246.9

Table 5 – Selected Monod kinetics for simulations.

Parameter	Symbol	Unit	Heterotrophic	Autotrophic
Maximum growth rate	$\mu_{max20°C}$	1/day	3	calibrated
Half-velocity coefficient, substrate	K_S	mg/L	20	N/A
Half-velocity coefficient, ammonia	K_N	mg-N/L	0.1	1.05
Half-velocity coefficient, DO	K_O	mg/L	0.5	1.0
Decay coefficient	K_D	1/day	0.06	0.06

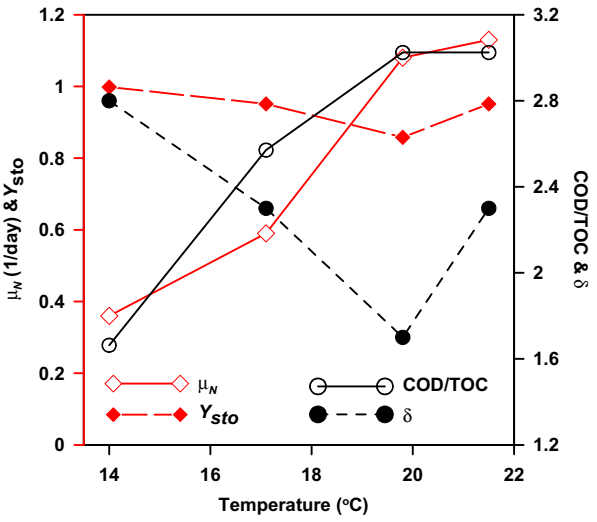

Fig. 4 – Calibrated parameter values at different testing temperatures.

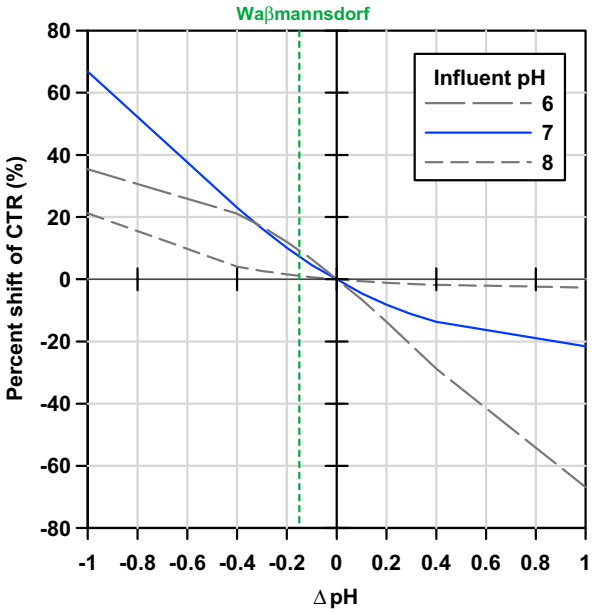

Fig. 5 – Effects of unexpected pH change to CPR simulations.

OTR plotted in the lowest panel of Fig. 2 showed the differences between CTR and OTR at different nitrification performance and degree of ammonia discharge: when the plant loads are under control and ammonia is fully nitrified, CTR matches well with OTR; but during times of high ammonia loading, CTR is lower than OTR (lower panel, shaded area).

Fig. 3 shows the correlations between CTR and OTR at the fully nitrified period versus the ammonia overloading period. This figure contains all the measurements of four testing periods and confirmed the higher OTR/CTR ratio during the ammonia overloading period. Off-gas measured OTRs and CTRs are linearly correlated, and the slope of OTR over CTR is higher at nitrogen overloading conditions. This differeces may be caused by two reasons: (1) when ammonia loads exceeded the nitrification capacity in the ASP, the heterotrophic organisms still consumed most of the carbonaceous substrate, producing the same amount of carbon dioxide, and used more oxygen for nitrification; (2) at peak flow, the additional influent alkalinity may shift the bicarbonate balance and reduce the CTR.

3.2. *Steady-state analysis*

Steady-state mass balance was performed to understand the relationship between bacteria activity, alkalinity balance, and gas transfer. Table 4 shows the fates of carbon (kg-C/hour) and

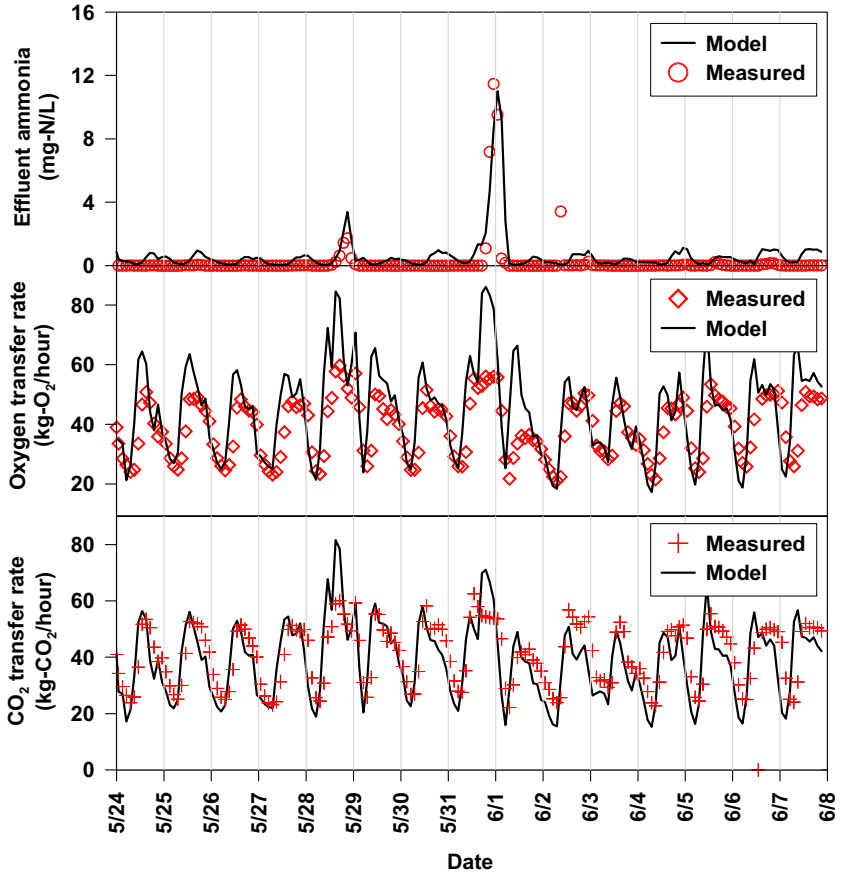

Fig. 6 – Simulation results of the three parameters (from top to bottom): effluent ammonia concentration, oxygen transfer rate, and carbon dioxide transfer rate. Activated sludge model was used to evaluate nitrification conditions.

oxygen (kg-O/hour) in the full-scale treatment process. The calculated total liquid phase CO_2 ($H_2CO_3^* + HCO_3-$) was 253.4 mg/L, and the saturated $H_2CO_3^*$ ($S^{\infty}_{H_2CO_3^*}$) was 54.7 mg/L (from off-gas CO_2). Based upon the two calculated concentrations, the fraction of HCO_3^- was estimated and confirmed with measured alkalinity and pH (6.80). The results showed that CO_2 was in equilibrium and the pH can be calculated. The oxygen content in the carbonaceous substrate (CH_xO_y) was also defined, whereas C:H:O = 1:1.5:0.48. This empirical formula was used in stoichiometry (Eqs. (4) and (5)) to calculate the yield coefficients (Table 2) for dynamic simulations.

3.3. *Model calibration and sensitivity analysis*

The model was calibrated partially by choosing from plausible parameters and others by comparing the simulations with measurement data. The standard maximum heterotrophic growth rates ($\mu_{max20^\circ C}$), cell decay rates (K_D), and half-velocity coefficients (K_N, K_S) are less sensitive for nitrification and CO_2 simulation; and the values of these parameters were chosen from well-defined empirical values from literatures (e.g. Metcalf and Eddy Inc., 2003), as shown in Table 5. For the other parameters, it is necessary to estimate the values for each season. Fig. 4 shows the calibrated values of the sensitive parameters, including the maximum nitrifier growth rate (μ_N), storage coefficient (δ), and COD/TOC ratio versus temperatures. For all the parameters the influences of temperatures are very significant: ammonia uptake rate and COD/TOC ratio increased dramatically with temperature, and the decrease of δ suggested that higher fraction of substrate uptake was used in direct synthesis then storage during summer.

A sensitivity analysis was performed to estimate the potential errors in CTR caused by changes of pH. The pH was varied from −1.0 to +1.0 units and the change in CTR was observed for three different influent pHs (6, 7, and 8, see Fig. 5). With no pH change, there is no error between predicted and actual CTR. If the pH decreases the model generally overestimates the CTR. For an increasing pH the model underestimates the CTR. Fig. 5 shows the error as a function of influent pH and change in aeration basin pH.

Based upon the proposed strategy, CTR can be calculated under the assumption that the change of pH (ΔpH in the figure) does not change dramatically in a short period. This will be a good assumption for treatment plants with high alkalinity wastewater, or wastewaters with low ammonia concentration or plants controlling pH. For the Waßmannsdorf plant, the pH was stable and the online measurements showed maximum pH change from 6.95 to 6.80, ΔpH = −0.15. The percent error in simulated and actual CTR due to this change of pH is small (~10%) and relatively constant, can be removed as a calibration factor. The good fit between simulated CTR and measurements at fully-nitrified period confirmed this hypothesis, as shown in Fig. 6.

3.4. *Results of dynamic simulation*

Fig. 6 shows an example of the simulated effluent ammonia, OTR, and CTR versus measured data during a monitoring period. The model successfully predicted the discharge of ammonia, and the simulated OTR and CTR generally fit with measured data after model calibration. The model predicted slightly higher OTR and lower DO (DO data not shown) than measured data during nitrogen overloading periods. The possible reason for this over-estimation of CTR and OTR could be due to the use of online measurements. During the nitrogen overloading period, measured oxygen supplied is lower than the calculated oxygen demand to consume all pollutants (substrate + ammonia). At constant DO, this difference in oxygen demands is characterized by using a lower $\alpha K_L a$, measured from off-gas tests; but when using the lower $\alpha K_L a$ in ASM, the model tends to underestimate DO and predicted slightly higher OTRs. This difference does not affect the accuracy in estimating OUR and the simulations of nitrification performance; the oxygen transferred in the system still equals the OUR plus the discharged DO.

In addition, the simulation results demonstrate that ammonia discharge is caused by nitrifying limitation due to plant operation (e.g., temperature, aeration volume, SRT) but not because of aeration failure, e.g. inadequate oxygen-transfer.

Based upon the simulation results, a control strategy to predict nitrification was proposed using off-gas monitoring data and an activated sludge model (see Fig. 7). The activated sludge model for different monitoring sections can be validated by periodic plant measurements and off-gas data. At certain period of each monitoring section, the model parameters can be validated using the demonstrated calibration procedure. At each section the calibrated model can be used to evaluate the dynamic ammonia consumption and predict the discharge with only information from off-gas monitoring,

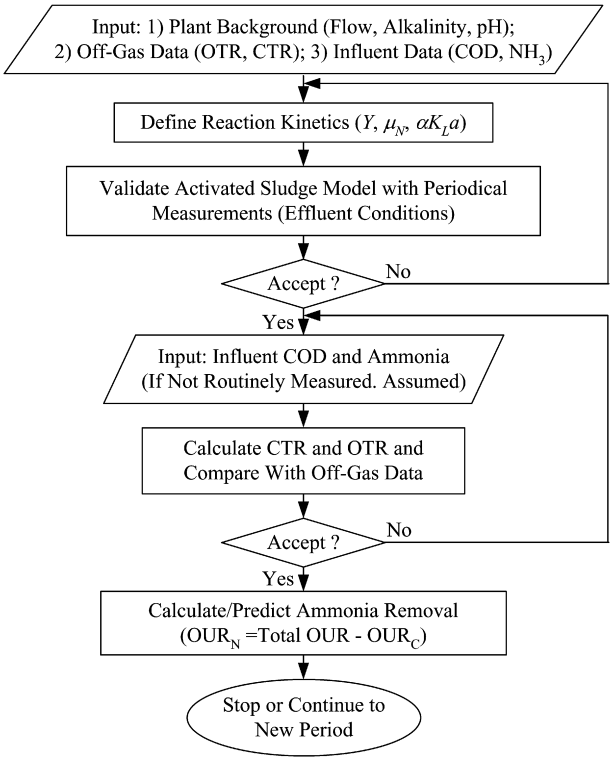

Fig. 7 – Block diagram of using off-gas monitoring and activated to estimate nitrification performance.

without needing information from frequently collected grab samples or other complex and costly online monitoring systems. Immediate response for the nitrogen discharge, such as effluent flow equalization or temperate increase of SRT, can be made based on the real-time monitoring results.

4. Conclusions

- This paper presented a strategy for using online off-gas O_2 and CO_2 monitoring to predict nitrification performance. The ratio of carbon dioxide transfer rate (CTR) to oxygen transfer rate (OTR) can be used to assess the relative rates of the heterotrophic and nitrifier communities. The ratio of the CTR to the OTR decreased during ammonia break through periods.
- The simulation results showed that rapid change of pH may significantly affect the accuracy of CTR estimation; but in a well controlled environment (i.e. aeration tank with pH control), the uncertainty may be reduced and become manageable by regular measurements of pH and alkalinity.
- Off-gas monitoring provides useful information to evaluate the nitrification status and off-gas CO_2 data can be valuable for model calibrations. The model successfully simulated CTR and was used to predict the ammonia discharge.
- Since both OTR and CTR can be measured in real-time with instruments that do not need to be in contact with the wastewater, a reliable on-line instrument could be developed to monitor nitrification efficiency.

Acknowledgements

This research was partially supported by the California Energy Commission and Southern California Edison Inc., a power company in California, U.S.A. The authors thank Anne Schuchardt and Chris Sahlmann for the data collection and water quality analysis.

Shao-Yuan Leu was a Ph.D. student at the time of the research, and is now a post-doctroal scholar and Michael K. Stenstrom is a professor in the Civil Engineering Department at the University of California, Los Angeles. Judy A. Libra is a researcher in the institute of Chemical Engineering, Technical University of Berlin, Germany. Correspondence should be addressed to M. K. Stenstrom, University of California Los Angeles, Dept. of Civil Engineering, 5714 Boelter Hall, Los Angeles, CA 90095-1593.

REFERENCES

American Society of Civil Engineering, 2006. ASCE Standard Measurement of Oxygen Transfer in Clean Water. ASCE 2-91, New York, NY.

American Society of Civil Engineering, 1997. Standard Guidelines for In-Process Oxygen Transfer Testing. ASCE 18-96, New York.

Clifft, R.C., Andrews, J.F., 1986. Gas-liquid interactions in oxygen activated sludge. J. Environ. Eng. 112 (1), 61–77.

Gujer, W., Henze, M., Mino, T., van Loosdrecht, M.C.M., 1999. Activated sludge model no. 3. Water Sci. Technol. 39 (1), 183–193.

Hellinga, C., Vanrolleghem, P., van Loosdrecht, M.C.M., Heijnen, J.J., 1996. The potential of off-gas analyses for monitoring wastewater treatment plants. Water Sci. Technol. 33 (1), 13–23.

Iranpour, R., Stenstrom, M.K., 2001. Relationship between oxygen transfer rate and airflow for fine-pore aeration under process conditions. Water Environ. Res. 73 (3), 266–275.

Krishna, C., van Loosdrecht, M.C.M., 1999. Substrate flux into storage and growth in relation to activated sludge modelling. Water Res. 33 (14), 3149–3161.

Leu, S.-Y., Rosso, D., Larson, L., Stenstrom, M.K., 2009. Real-time aeration efficiency monitoring in the activated sludge process and methods to reduce energy consumption and operating costs. Water Environ. Res. 81 (12), 2471–2481.

Lewis, W.K., Whitman, W.G., 1924. Principles of gas absorption. Ind. Eng. Chem. 16 (12), 1215–1220.

Metcalf and Eddy Inc., 2003. In: Wastewater Engineering: Treatment, Disposal, Reuse, fourth ed. McGraw-Hill, New York, NY.

Minkevich, I.G., Neubert, M., 1985. Influence of carbon dioxide solubility on the accuracy of measurements of carbon dioxide production rate by gas balance technique. Acta Biotechnol. 5, 137–143.

Nogita, S., Watanabe, S., Baba, K., 1982. Basic studies on carbon dioxide/air control system for activated sludge processes. Water Res. 16 (6), 1017–1024.

Painter, H.A., 1970. A review of literature on inorganic nitrogen metabolism in microorganisms. Water Res. 4, 393–450.

Painter, H.A., Loveless, J.E., 1983. Effect of temperature and pH value on the growth-rate constants of nitrifying bacteria in the activated sludge process. Water Res. 17, 238–248.

Poduska, R.A., Andrews, J.F., 1975. Dynamics of nitrification in the activated sludge process. J. Water Pollut. Control Fed. 47 (11), 2599–2619.

Pratt, S., Yuan, Z., Gapse, D., Dorigo, M., Zeng, R., Keller, J., 2003. Development of a novel titration and off-gas analysis (TOGA) sensor for study of biological processes in wastewater treatment systems. Biotechnol. Bioeng. 81 (4), 482–495.

Pratt, S., Yuan, Z., Keller, J., 2004. Modeling aerobic carbon oxidation and storage by integrating respirometric, titrimetric, and off-gas CO_2 measurements. Biotechnol. Bioeng. 88 (2), 135–147.

Redmon, D.T., Boyle, W.C., Ewing, L., 1983. Oxygen transfer efficiency measurements in mixed liquor using off-gas techniques. J. Water Pollut. Control Fed. 55, 1338–1347.

Rosso, D., Iranpour, R., Stenstrom, M.K., 2005. Fifteen years of off-gas transfer efficiency measurements on fine pore aerators: key role of sludge age and normalized air flux. Water Environ. Res. 77 (3), 266–273.

Schuchardt, A., Libra, J.A., Sahlmann, C., Handschag, J., Wiesmann, U., Gnirss, R., 2005. Potential of OUR and OTR measurements for identification of activated sludge removal processes in aerated basins. Water Sci. Technol. 52 (12), 141–149.

Sin, G., Guisasola, A., De Pauw, D.J.W., Baeza, J.A., Carrera, J., Vanrolleghem, P.A., 2005. A new approach for modelling simultaneous storage and growth processes for activated sludge systems under aerobic conditions. Biotechnol. Bioeng. 92 (5), 600–613.

Spérandio, M., Paul, E., 1997. Determination of carbon dioxide evolution rate using on-line gas analysis during dynamic biodegradation experiments. Biotechnol. Bioeng. 53 (3), 243–252.

Stenstrom, M.K., Poduska, R.A., 1980. The effect of dissolved oxygen concentration on nitrification. Water Res. 14 (6), 643–649.

Stenstrom, M.K., Song, S., 1991. Effects of mass transport limitation on nitrification in the activated sludge process. Research J. WPCF 63 (3), 208–219.

Stenstrom, M.K., Kido, W., Shanks, R.F., Mulkerin, M., 1989. Estimating oxygen transfer capacity of a full-scale pure oxygen activated sludge plant. Research J. WPCF 61 (2), 208–220.

Weissenbacher, N., Lenz, K., Mahnik, S., Wett, B., Fuerhacker, M., 2006. Determination of activated sludge biological activity using model corrected CO_2 off-gas data. Water Res. 41 (7), 1587–1595.

Tzeng, C.J., Iranpour, R., Stenstrom, M.K., 2003. Modeling and control of oxygen transfer in the HPO activated sludge process. J. Environ. Eng., ASCE 129 (5), 402–411.

Yuan, W., Okrent, D., Stenstrom, M.K., 1993. Model calibration for the high-purity oxygen activated sludge process – algorithm development and evaluation. Water Sci. Technol. 28 (11, 12), 163–171.